Electronic Supplementary Material (ESI) for Nanoscale.

Supplementary Information for
Multivalent non-covalent interactions lead to strongest polymer adhesion

Max Lallemang[a,b], Leixiao Yu[c], Wanhao Cai[a], Klaus Rischka[d], Andreas Hartwig[d,e], Rainer Haag[c], Thorsten Hugel[a,b,*], Bizan N. Balzer[a,b,f,*]

[a]*Institute of Physical Chemistry, University of Freiburg, Albertstraße 21, 79104 Freiburg, Germany.*

[b]*Cluster of Excellence livMatS @ FIT-Freiburg Center for Interactive Materials and Bioinspired Technologies, University of Freiburg, Georges-Köhler-Allee 105, 79110 Freiburg, Germany*

[c]*Institute of Chemistry and Biochemistry, Freie Universität Berlin, Takusstraße 3, 14195 Berlin, Germany*

[d]*Fraunhofer Institute for Manufacturing Technology and Advanced Materials IFAM, Wiener Straße 12, 28359 Bremen, Germany*

[e]*University of Bremen, Department 2 Biology/Chemistry, Leobener Straße 3, 28359 Bremen, Germany*

[f]*Freiburg Materials Research Center (FMF), Albert Ludwig University of Freiburg, 79104 Freiburg, Germany*

* Bizan N. Balzer, Thorsten Hugel.

Email: bizan.balzer@physchem.uni-freiburg.de, thorsten.hugel@physchem.uni-freiburg.de

This PDF file includes:

1. AFM cantilever tip functionalization

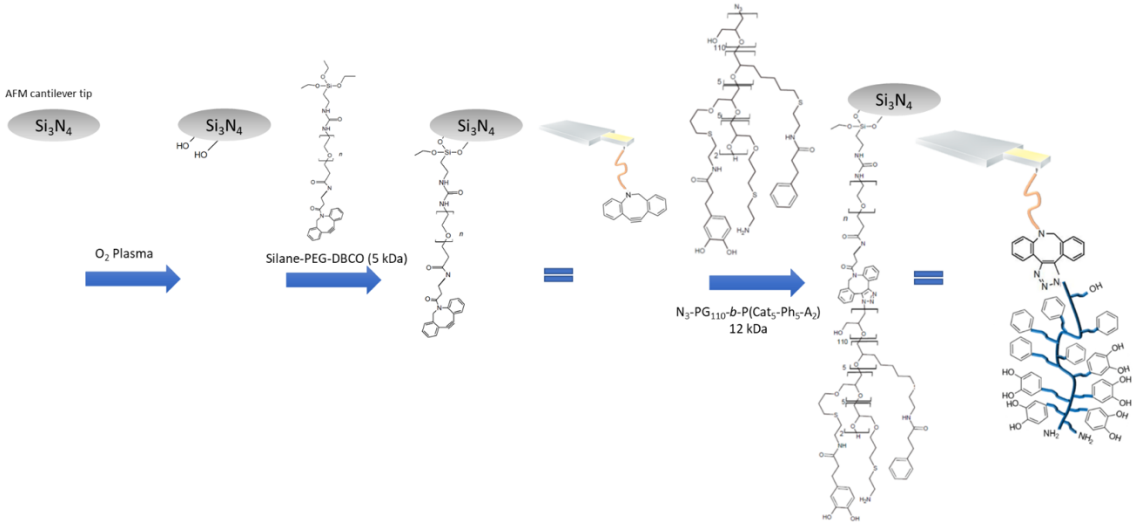

Fig. S1. Functionalization of an AFM cantilever tip. To obtain a covalently bound PG_{110}-*b*-P(Cat_5-Ph_5-A_2) molecular force sensor, oxygen plasma treatment, silane-PEG-DBCO (5 kDa) and N_3-PG_{110}-*b*-P(Cat_5-Ph_5-A_2) (12 kDa) were used.

2. Contact angle measurements

To further characterize the presence of N_3-PG_{110}-*b*-P(Cat_5-Ph_5-A_2) layers on a TiO_2 substrate, contact angle measurements were performed using a homebuilt goniometer. The control samples were TiO_2 incubated in the pure solvent (MOPS buffer pH 6.0, 0.1 M) instead of the polymer solution. Ten droplets of H_2O (1 µL) were put on each layer. For each droplet, the contact angle was determined using the distance tool of the software *Gwyddion 2.47*.[1] Finally, the average value and standard deviation were calculated (Fig. S2). The presence of N_3-PG_{110}-*b*-P(Cat_5-Ph_5-A_2) layers increased the hydrophilicity and therefore the contact angle became smaller.

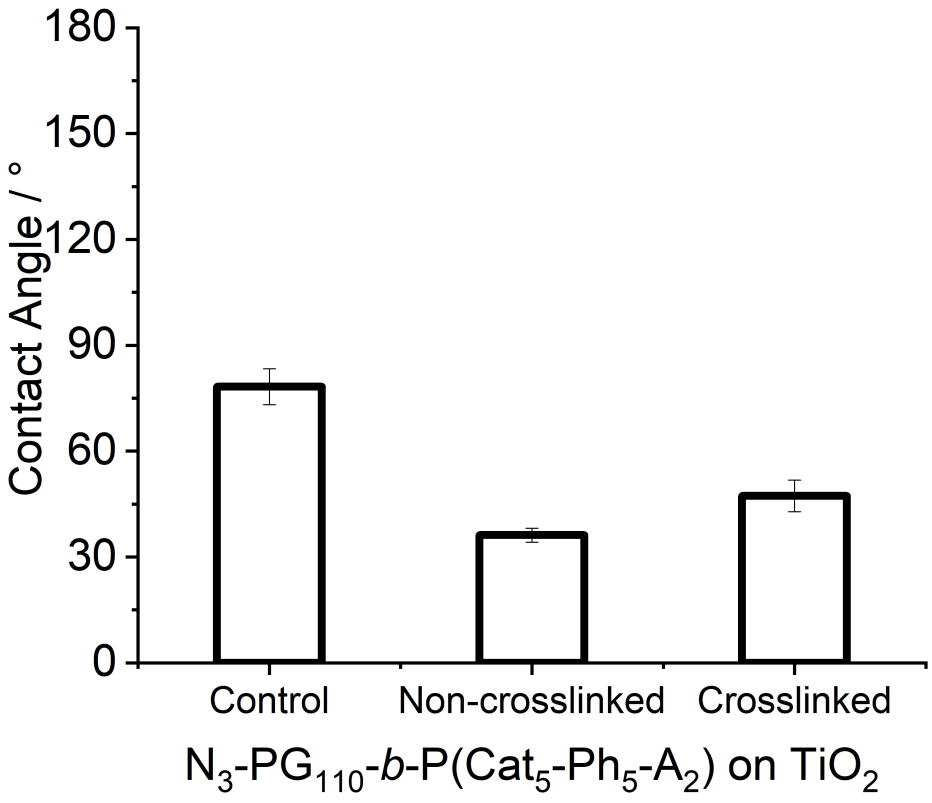

Fig. S2. Contact angle measurements of a non-crosslinked N_3-PG_{110}-*b*-P(Cat_5-Ph_5-A_2) layer on TiO_2, a crosslinked N_3-PG_{110}-*b*-P(Cat_5-Ph_5-A_2) layer on TiO_2 and bare TiO_2 as a control. The control samples on TiO_2 were incubated in the pure solvent (MOPS buffer pH 6.0, 0.1 M) instead of the polymer solution. The contact angles amounted to (78 ± 5) ° for the control, (36 ± 2) ° for the non-crosslinked layer and (47 ± 5) ° for the crosslinked layer.

3. Thickness determination of a N_3-PG_{110}-*b*-P(Cat_5-Ph_5-A_2) layer on TiO_2 by AFM-based scratching

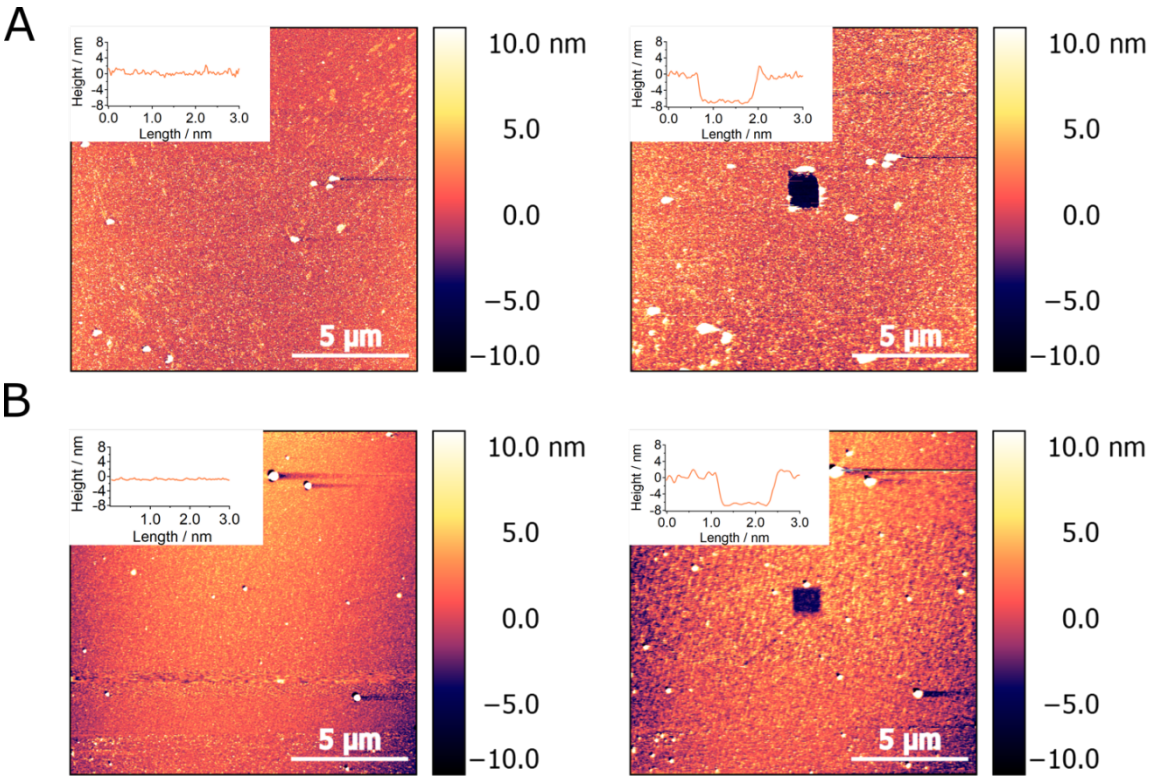

Fig. S3. Scratching of a N_3-PG_{110}-*b*-P(Cat_5-Ph_5-A_2) layer on TiO_2. Imaging of the layer with a scan size of 15•15 µm^2 (left). Imaging of the layer after the scratch with a scan size of 15•15 µm^2 (right). A scan rate of 2 Hz was used for all images. **A.** The thickness of a non-crosslinked N_3-PG_{110}-*b*-P(Cat_5-Ph_5-A_2) layer on TiO_2 in buffer (pH 6.0) amounted to (8.5 ± 0.7) nm. **B.** A crosslinked layer on TiO_2 in buffer (pH 6.0) showed a thickness of (6.8 ± 0.9) nm.

4. Force spectroscopy

4a. PG_{110}-*b*-P(Cat_5-Ph_5-A_2) molecular force sensor on SiO_2

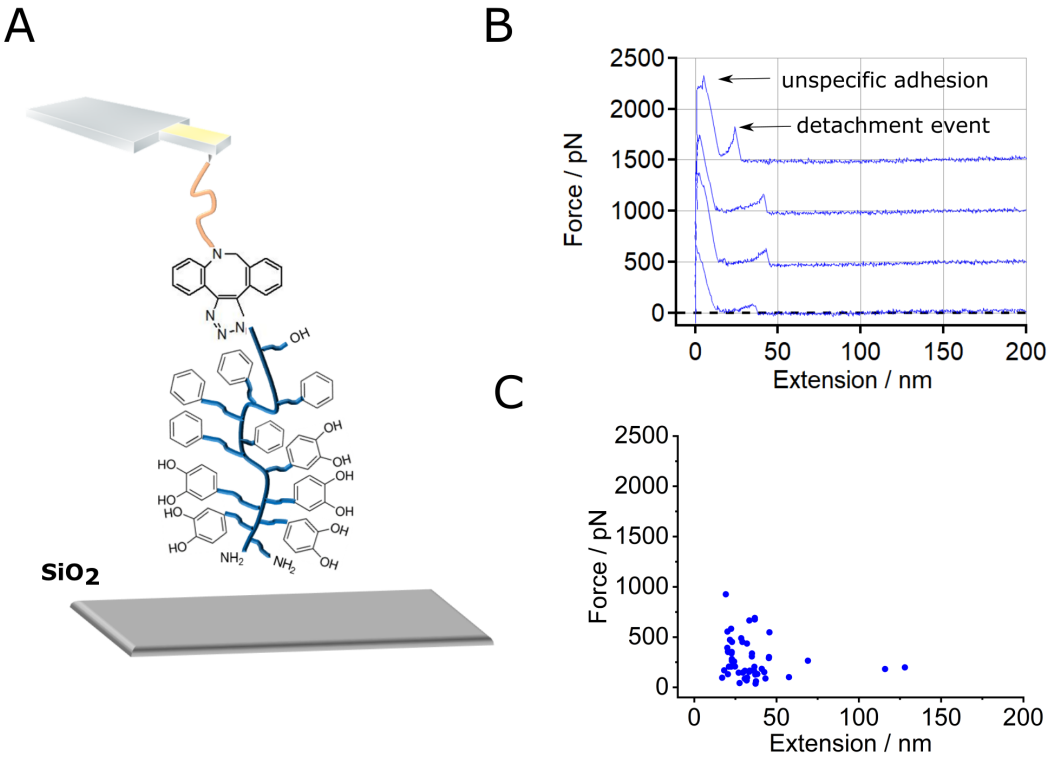

Fig. S4. PG_{110}-*b*-P(Cat_5-Ph_5-A_2) molecular force sensor on SiO_2. A. Scheme of the experiment. An AFM cantilever tip was functionalized with silane-PEG-DBCO (linker) and N_3-PG_{110}-*b*-P(Cat_5-Ph_5-A_2) and measured on SiO_2 in H_2O with a contact force of 500 pN and a contact time of 1 s. **B.** Representative force-extension curves. Out of 200 force-extension curves, 40 showed convex stretch events (20 %), 6 curves showed double convex stretches (3 %) and 5 curves showed multiple stretches (3 %). There were no concave stretches or plateaus. The curves were offset by 500 pN for graphical presentation. **C.** Scatter plot showing the detachment force distribution (including all peaks except unspecific adhesion) vs the detachment position. The average detachment force showed a value of (276 ± 192) pN and the average detachment position a value of (34 ± 20) nm.

4b. PEG-DBCO molecular force sensor on SiO_2

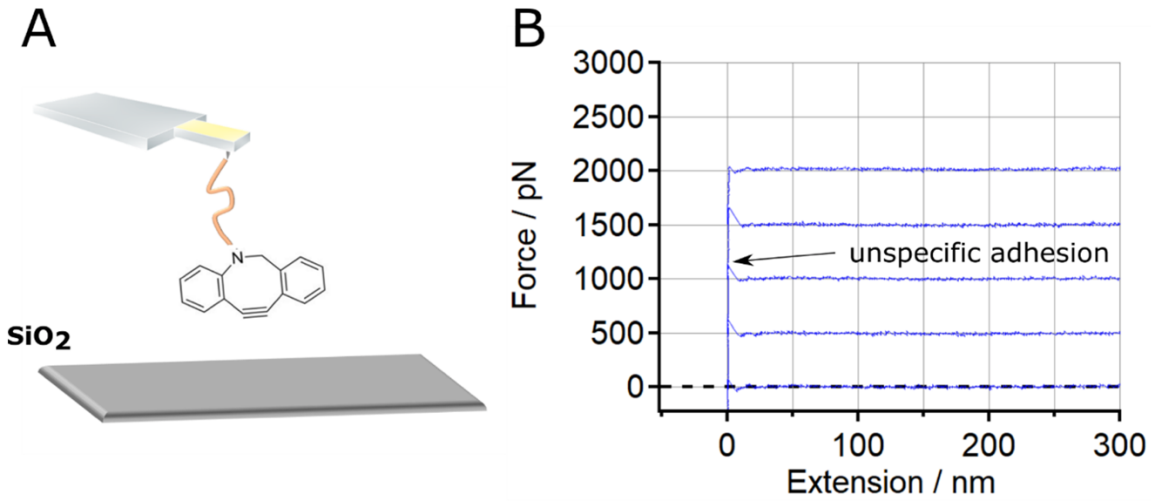

Fig. S5. PEG-DBCO molecular force sensor on SiO_2. A. Scheme of the experiment. An AFM cantilever was functionalized with silane-PEG-DBCO and measured on SiO_2 in H_2O with a contact force of 500 pN and a contact time of 1 s. **B.** Force-extension curves of silane-PEG-DBCO on SiO_2. Out of 200 curves, there were no curves with concave or convex stretches or plateaus. The curves were offset by 500 pN for graphical presentation.

4c. Contact force vs contact time for a PG_{110}-*b*-P(Cat_5-Ph_5-A_2) molecular force sensor on a N_3-PG_{110}-*b*-P(Cat_5-Ph_5-A_2) layer on TiO_2

In order to understand the timescales involved in the formation of bonds between a PG_{110} - *b*-P(Cat_5-Ph_5-A_2) molecular force sensor and a N_3-PG_{110}-*b*-P(Cat_5-Ph_5-A_2) layer on TiO_2, we varied the contact time of the molecular force sensor on the layer and the contact force with which the AFM cantilever tip was pressed against this layer (Fig. S6).
As a control, we started with a contact force of 50 pN (below the breakthrough force) with contact times of 0 s, 1 s and 10 s. The real contact time (comprising dwell and contact during approach and retract of the AFM cantilever tip) for 0 s is 0.02 s for 50 pN, 0.05 s for 500 pN and 0.09 s for 3000 pN. For 1 s, the real contact times are 1.02 s for 50 pN, 1.04 s for 500 pN and 1.09 s for 3000 pN. Finally, a contact time of 10 s means a real contact time of 10.02 s for 50 pN, 10.04 s for 500 pN and 10.07 s for 3000 pN.
The experiments with a contact force of 50 pN only showed force-extension curves with low detachment forces in the range of 100 pN (Fig. S7). Only an increase of the contact force to 500 pN (above the breakthrough force) led to a noticeable increase in the detachment forces, reaching values greater than 2000 pN (Fig. S7). This is in accordance with the repelling properties assigned to N_3-PG_{110}-*b*-P(Cat_5-Ph_5-A_2) layers.[2]
Increasing the contact force further to a value of 3000 pN revealed diverse types of force-extension curves (see also Fig. 1d). We interpret this as a higher probability for the interactions between the functional groups of PG_{110}-*b*-P(Cat_5-Ph_5-A_2) on the AFM cantilever tip and the N_3-PG_{110}-*b*-P(Cat_5-Ph_5-A_2) layer. In that respect, we observed a significant amount of desorption plateaus as well as multiple plateaus. The highest number of convex stretches (35 %) was obtained for a contact time of 10 s and a contact force of 3000 pN. We believe that the increase of contact time results in a strengthening of the interactions between catechol groups of the PG_{110}-*b*-P(Cat_5-Ph_5-A_2) molecular force sensor and the N_3-PG_{110}-*b*-P(Cat_5-Ph_5-A_2) layer. Indentation curves as the one given in Figure 1c, reveal that contact forces of at least 200 to 400 pN were necessary for a characteristic break-through of the N_3-PG_{110}-*b*-P(Cat_5-Ph_5-A_2) layer.
Based on these results, we chose a contact time of 1 s and a contact force of 500 pN as threshold values for further measurements, which is a good compromise between monitoring a great number of interactions and preventing a too high number of overlapping interactions (resulting in overlapping detachment events) rendering the force-extension curves uninterpretable.

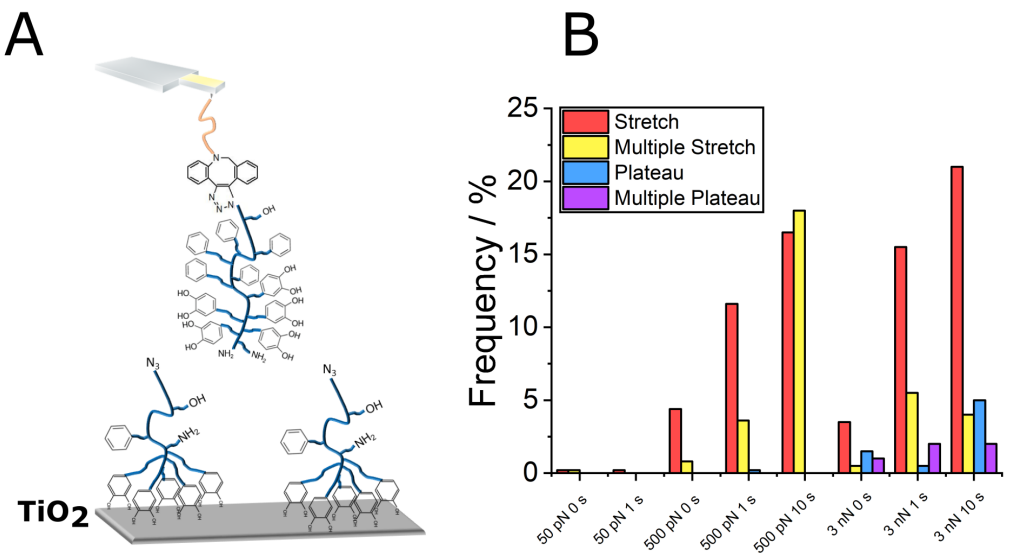

Fig. S6. Effect of contact force and contact time for a PG_{110}-*b*-$P(Cat_5$-Ph_5-$A_2)$ molecular force sensor on a non-crosslinked N_3-PG_{110}-*b*-$P(Cat_5$-Ph_5-$A_2)$ layer on TiO_2. A. Scheme of a PG_{110}-*b*-$P(Cat_5$-Ph_5-$A_2)$ molecular force sensor on a non-crosslinked N_3-PG_{110}-*b*-$P(Cat_5$-Ph_5-$A_2)$ layer on TiO_2. **B.** Frequency of the different curve types, showing stretches, multiple stretches, plateaus and multiple plateaus is given for different contact forces (50 pN, 500 pN, 3000 pN) and different contact times (0 s, 1 s, 10 s). The experiments were performed in H_2O. The frequency has been scaled to the total number of curves taken (200 for each condition).

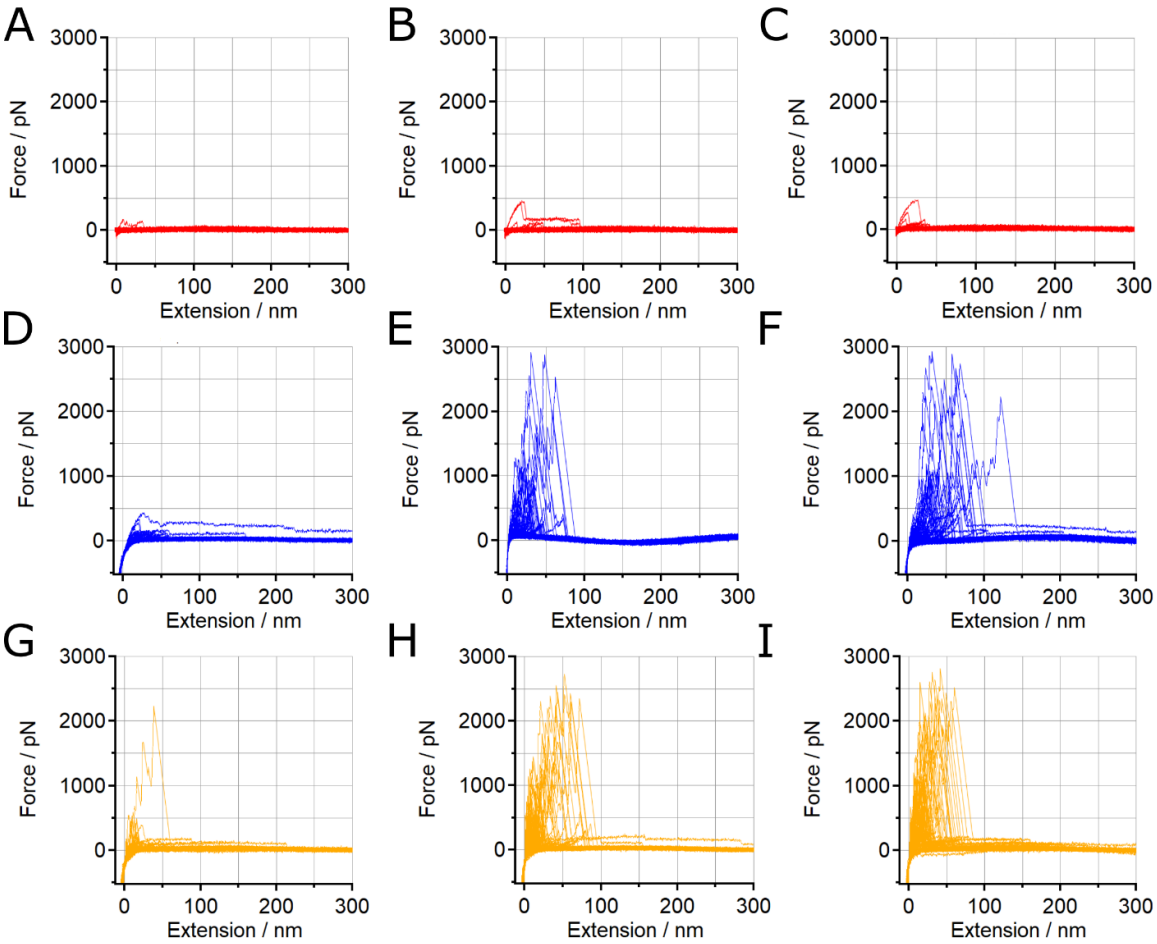

Fig. S7. PG_{110}-*b*-P(Cat_5-Ph_5-A_2) molecular force sensor on a N_3-PG_{110}-*b*-P(Cat_5-Ph_5-A_2) layer on TiO_2 with different contact forces (50 pN, 500 pN, 3000 pN) and different contact times (0 s, 1 s, 10 s) measured in H_2O. A. 50 pN, 0 s **B**. 50 pN, 1 s **C**. 50 pN, 10 s **D**. 500 pN, 0 s, **E**. 500 pN, 1 s, **F**. 500 pN, 10 s, **G**. 3000 pN, 0 s, **H**. 3000 pN, 1 s, **I**. 3000 pN, 10 s.

4d. Force-extension curves with forces higher than 1500 pN

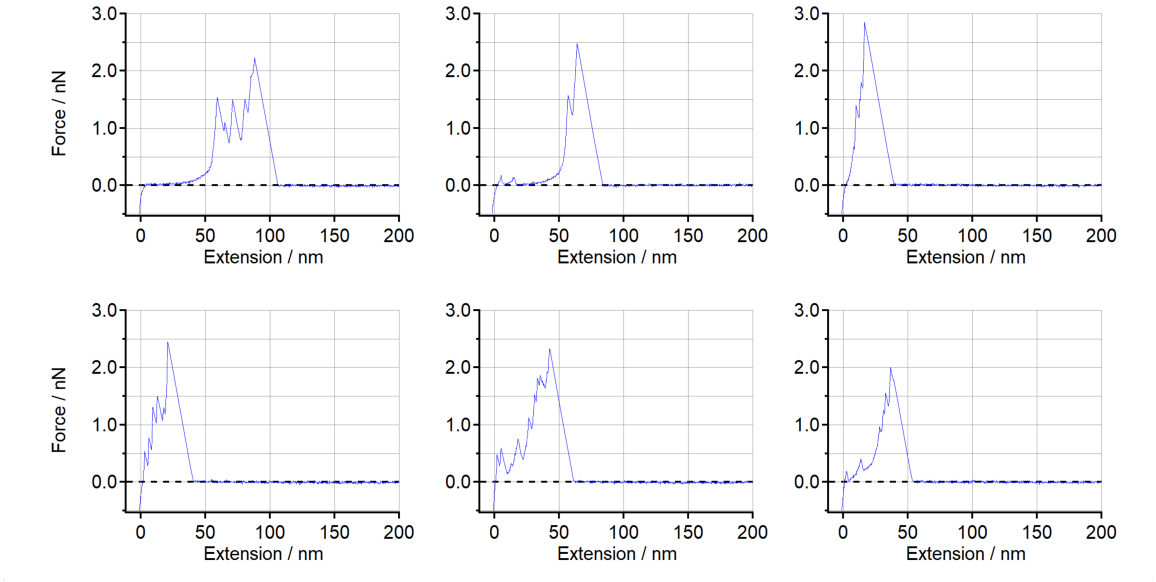

Fig. S8. Exemplary force-extension curves for a PG_{110}-*b*-P(Cat_5-Ph_5-A_2) molecular force sensor on a N_3-PG_{110}-*b*-P(Cat_5-Ph_5-A_2) layer on TiO_2 with detachment forces higher than 1500 pN. These force-extension curves were taken at the condition pH 8.6 crosslinked.

4e. Frequency of different force-extension motifs for a PG_{110}-*b*-P(Cat_5-Ph_5-A_2) molecular force sensor on a N_3-PG_{110}-*b*-P(Cat_5-Ph_5-A_2) layer on TiO_2

The different types of force-extension curves for a PG_{110}-*b*-P(Cat_5-Ph_5-A_2) molecular force sensor on a N_3-PG_{110}-*b*-P(Cat_5-Ph_5-A_2) layer on TiO_2 are listed in Table S1. The numbers indicate the absolute number of a certain type of detachment event, while the numbers in the brackets indicate the respective frequency of occurrence in % with respect to the total number of force-extension curves taken.

Table S1. Number (frequency of occurrence) of the different force-extension curves for a PG_{110}-*b*-P(Cat_5-Ph_5-A_2) molecular force sensor on a N_3-PG_{110}-*b*-P(Cat_5-Ph_5-A_2) layer on TiO_2.

Condition		pH 6.0	pH 8.6	pH 8.6 crosslinked
Number of events	Concave stretch	5 (1 %)	0 (0 %)	0 (0%)
	Convex stretch	72 (14 %)	110 (21 %)	89 (17 %)
	Double convex stretch	11 (2 %)	39 (8 %)	23 (4 %)
	Multiple stretch	39 (8 %)	35 (7 %)	15 (3 %)
	Single plateau	3 (1 %)	0 (0 %)	1 (1 %)
	Multiple plateaus	1 (1 %)	0 (0 %)	0 (0 %)

4f. Number of detachment events for a PG_{110}-*b*-P(Cat_5-Ph_5-A_2) molecular force sensor on a N_3-PG_{110}-*b*-P(Cat_5-Ph_5-A_2) layer on TiO_2

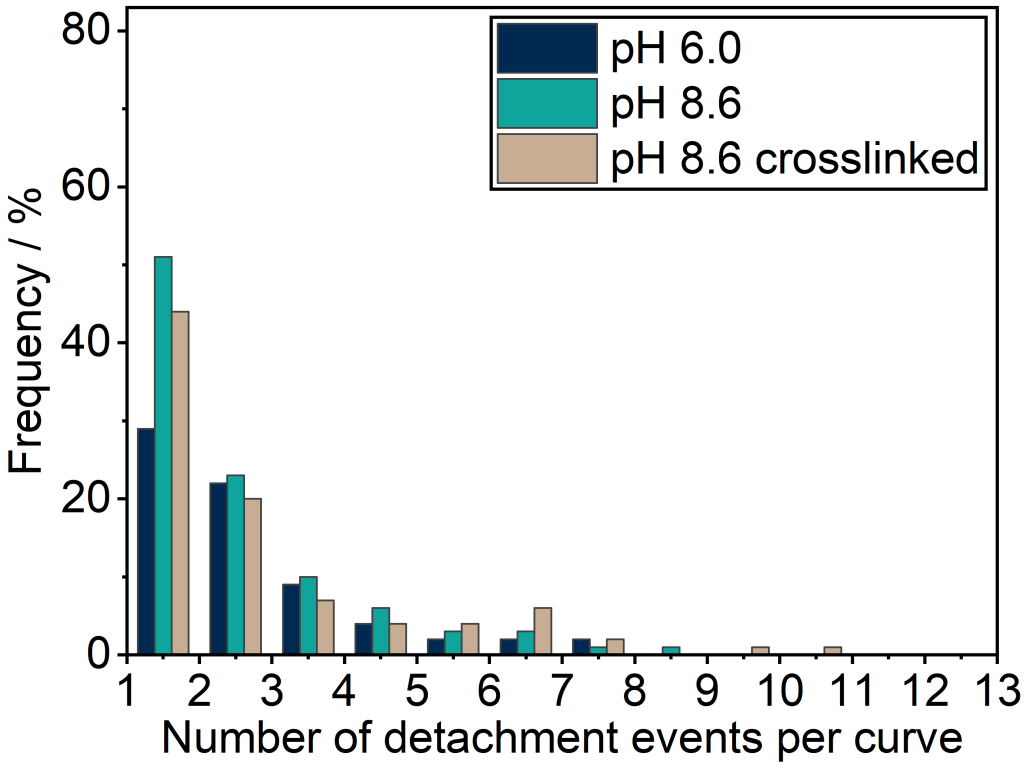

Fig. S9. Number of detachment events per curve. For a PG_{110}-*b*-P(Cat_5-Ph_5-A_2) molecular force sensor on a N_3-PG_{110}-*b*-P(Cat_5-Ph_5-A_2) layer on TiO_2 the following number of force-extension curves was obtained: 70 at pH 6.0, 98 at pH 8.6 and 89 at pH 8.6 crosslinked.

4g. Average energy per peak

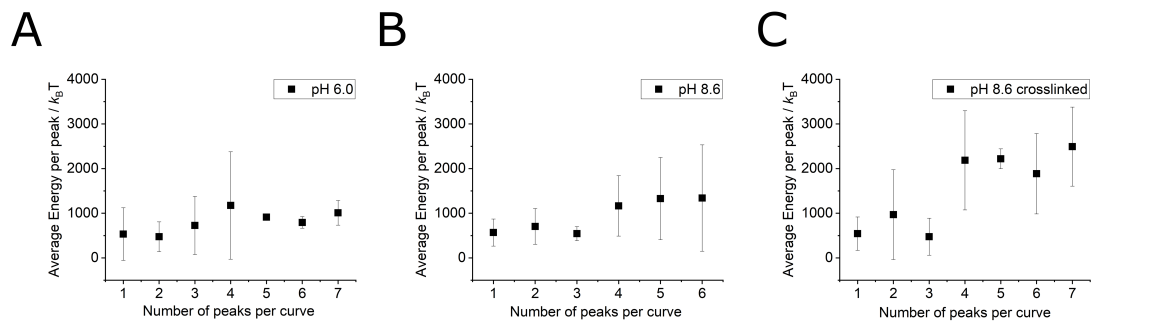

Fig. S10. Average energy per peak as a function of the number of peaks per curve. A PG_{110} - *b*-P(Cat_5-Ph_5-A_2) molecular force sensor on a N_3-PG_{110}-*b*-P(Cat_5-Ph_5-A_2) layer on TiO_2 is shown for pH 6.0 (A), pH 8.6 (B) and pH 8.6 (C) crosslinked. The area between the force-extension curve and the baseline were determined by a trapezoidal integration.

SI References

1. D. Nečas, P. Klapetek, Gwyddion: an open-source software for SPM data analysis. *Open Physics* 10, 181-188 (2012).
2. L. Yu, C. Cheng, Q. Ran, C. Schlaich, P.-L. M. Noeske, W. Li, Q. Wei and R. Haag, Bioinspired Universal Monolayer Coatings by Combining Concepts from Blood Protein Adsorption and Mussel Adhesion, *ACS Appl. Mater. Interfaces* 9, 6624-6633 (2017).